JCI insight

Human IL-6 fosters long-term engraftment of patient derived disease-driving myeloma cells in immunodeficient mice

Zainul S. Hasanali, … , Edward A. Stadtmauer, David Allman

JCI Insight. 2024. https://doi.org/10.1172/jci.insight.177300.

Resource and Technical Advance In-Press Preview Hematology

Multiple myeloma is a largely incurable and life-threatening malignancy of antibody-secreting plasma cells. An effective and widely available animal model that recapitulates human myeloma and related plasma cell disorders is lacking. We show that busulfan-conditioned hIL-6 transgenic NSG mice (NSG+hIL6) reliably support the engraftment of malignant and pre-malignant human plasma cells including from patients diagnosed with monoclonal gammopathy of undetermined significance, pre- and post-relapse myeloma, plasma cell leukemia, and AL amyloidosis. Consistent with human disease, NSG+hIL6 mice engrafted with patient-derived myeloma cells, developed serum M spikes, and a majority developed anemia, hypercalcemia, and/or bone lesions. Single cell RNA sequencing showed non-malignant and malignant cell engraftment, the latter expressing a wide array of mRNAs associated with myeloma cell survival and proliferation. Myeloma engrafted mice given CAR T-cells targeting plasma cells or bortezomib experienced reduced tumor burden. Our results established NSG+hIL6 mice as an effective patient derived xenograft model for study and preclinical drug development of multiple myeloma and related plasma cell disorders.

Human IL-6 fosters long-term engraftment of patient derived disease-driving myeloma cells in immunodeficient mice

Zainul S. Hasanali[1], Alfred L. Garfall[1], Lisa Burzenski[2], Leonard D. Shultz[2], Yan Tang[3], Siddhant Kadu[3], Neil C. Sheppard[3,5], Wei Liu[3], Derek Dopkin[4], Dan T. Vogl[1], Adam D. Cohen[1], Adam J. Waxman[1], Sandra P. Susanibar-Adaniya[1], Martin Carroll[1,4], Edward A. Stadtmauer[1], and David Allman[5]

Affiliations:

[1] Division of Hematology Oncology, University of Pennsylvania, Philadelphia, PA, USA 19104

[2] Jackson Laboratories, Bar Harbor, ME, USA 04609

[3] Center for Cellular Immunotherapies, University of Pennsylvania, Philadelphia, PA, USA 19104

[4] Stem Cell and Xenograft Core Facility, University of Pennsylvania, Philadelphia, PA, USA 19104

[5] Department of Pathology and Laboratory Medicine, Perelman School of Medicine, University of Pennsylvania, Philadelphia, PA, USA 19104

Address correspondence to ZSH (Zainul.Hasanali@pennmedicine.upenn.edu) and DA (dallman@pennmedicine.upenn.edu), phone number: 215 746 5547.

ALG -Consulting from Janssen, BMS/Celgene, Novartis, Abbvie, GSK, DSMB membership for Janssen. Research funding from Janssen, Novartis, CRISPR Therapeutics and Tmunity Therapeutics.

NCS - Holds equity in Tmunity Therapeutics.

DTV -Consulting for Takeda, Abbvie, Sanofi/Genzyme, Genentech/Roche, Karyopharm and CSL/Behring. Research funding from Takeda and Active Biotech.

ADC -Consulting for Janssen, GSK, BMS/Celgene, Genentech/Roche, Pfizer, Abbvie, Arcellx, Ichnos, Takeda. Research funding from Novartis, GSK, Genentech. Patents in CART cell therapy with Novartis.

EAS -Consulting for Janssen and BMS/Celgene. Research funding from Sorrento and Abbvie.

Remaining authors have no conflicts of interest to disclose.

Abstract

Multiple myeloma is a largely incurable and life-threatening malignancy of antibody-secreting plasma cells. An effective and widely available animal model that recapitulates human myeloma and related plasma cell disorders is lacking. We show that busulfan-conditioned hIL-6 transgenic NSG mice (NSG+hIL6) reliably support the engraftment of malignant and pre-malignant human plasma cells including from patients diagnosed with monoclonal gammopathy of undetermined significance, pre- and post-relapse myeloma, plasma cell leukemia, and AL amyloidosis. Consistent with human disease, NSG+hIL6 mice engrafted with patient-derived myeloma cells, developed serum M spikes, and a majority developed anemia, hypercalcemia, and/or bone lesions. Single cell RNA sequencing showed non-malignant and malignant cell engraftment, the latter expressing a wide array of mRNAs associated with myeloma cell survival and proliferation. Myeloma engrafted mice given CAR T-cells targeting plasma cells or bortezomib experienced reduced tumor burden. Our results established NSG+hIL6 mice as an effective patient derived xenograft model for study and preclinical drug development of multiple myeloma and related plasma cell disorders.

Introduction

Multiple myeloma (MM) and related clonal bone marrow (BM) plasma cell dyscrasias (PCDs) cause ~100,000 deaths/year worldwide (1). In addition to MM, these disorders include a pre-malignant state called monoclonal gammopathy of undetermined significance (MGUS) (2), a highly aggressive and therapy resistant leukemia termed plasma cell leukemia (PCL) (3) and AL amyloidosis, which is characterized by the formation of monoclonal antibody-driven amyloid fibrils (4). Despite substantial recent advances in therapy options for MM, PCL, and AL amyloidosis patients that build on the previous success of proteasome inhibitors and thalidomide analogs (5, 6), the majority of patients experience relapse and eventually succumb to complications of treatment-refractory disease (7).

A major roadblock to curative drug development for myeloma and other PCDs has been the lack of a flexible and readily accessible animal model that recapitulates human disease. In principle, any such model would support the long-term persistence and growth of primary patient derived PCDs in a manner that mirrors both the growth properties of PCDs and key clinical signs such as anemia, hypercalcemia, renal damage, and bone destruction. Currently, the standard approach to study novel therapeutics in vivo is in immunodeficient mice engrafted with MM cell lines (8-10). However, cell line xenograft models fail to reliably recapitulate many aspects of clinical disease, do not faithfully model drug resistance mechanisms, and the cell lines used often grow aggressively, in contrast to most slower growing PCDs (11, 12). An alternative approach involves engraftment of human fetal or rabbit bone chips implanted into immunodeficient mice; however, these systems fail to drive clinical signs of disease, and the bone-resident MM cells do not disseminate throughout the skeleton as the disease does in humans (13).

Two patient derived xenograft models have been reported for primary myeloma. The first uses NSG mice in a similar approach to that presented here (14). However, prolonged engraftment, characterization of engrafted cells, characterization of clinical phenotypes and evaluation of cellular immunotherapies have not been performed. The second, from Das *et al.,* showed that immunodeficient

mice (RAG2$^{-/-}$ γc$^{-/-}$) harboring humanized versions of several cytokines including G-CSF, GM-CSF, IL-3 and IL-6 (MISTRG6) afford robust engraftment of patient PCDs (15). Though Das *et al*. determined that IL-6 is essential for PCD engraftment, the necessity of the other humanized genes was not firmly established. This more complex model is also difficult to obtain due to licensing restrictions and requires continuous antibiotic administration, resulting in limited use within the myeloma research community.

We studied the engraftment and long-term persistence of all major PCDs after transfer into transgenic NSG mice harboring a bacterial artificial chromosome (BAC) containing the human IL-6 gene (NSG+huIL6). We reasoned that increasing systemic IL-6 levels with a humanized BAC might be advantageous, because the BAC is likely to contain cis-regulatory elements needed for proper cell-type restricted IL-6 expression and because mouse IL-6 does not stimulate the human IL-6 receptor (16). Our results establish NSG+hIL6 mice as a straightforward and readily accessible system for the study of a wide range of PCD disease manifestations and therapies including newly diagnosed and relapsed myeloma.

Results

NSG+hIL6 transgenic mice were generated by microinjecting a BAC containing the promoter and gene elements of the human IL-6 gene on chromosome 7 into fertilized embryos of NSG mice (17). Because heterozygous females had low fertility, we bred males with normal NSG females; ~50% of the resulting pups carried the BAC. ELISA analyses showed that the majority of NSG+hIL6 mice possessed human IL-6 (mean 246.3 pg/mL, range 0-1020) in sera. hIL-6 levels distributed into two groups, 9-300pg/mL and 300-600pg/mL (**Figure 1**). There were no associations or trends observed in downstream experiments between the two groups. These IL-6 levels are higher than those observed in normal human sera (<5pg/mL) (18), yet they are in the range of IL-6 expression in PCDs (0.01-4ng/mL) (19).

Patient MM cell engraftment in NSG+hIL6 mice

Using established xenotransplantation protocols (20), we examined the impact of host pre-conditioning with busulfan with and without the presence of the human IL6 locus on engraftment of primary MM cells following intraosseous injection of T cell depleted patient BM mononuclear cells. Initially we tested for engraftment of malignant plasma cells from two new diagnosis MM patients (MM1 and MM2) following transfer of $1x10^6$ mononuclear BM cells per mouse. We evaluated human antibodies in sera every 5 weeks out to 20 weeks post-transfer and then at 52 weeks post-transfer. Within 5 weeks we readily detected human Ig in sera in busulfan treated NSG+hIL6 mice for both MM1 and MM2. By contrast, at this time, engraftment was far less routine for busulfan treated NSG mice and NSG+hIL6 mice without busulfan (**Figure 2A**). Furthermore, for most pre-conditioned NSG+hIL6 mice, serum titers for human Ig increased progressively over 20 weeks (**Figure 2B**). Time to engraftment was defined by the initial detection of human Ig in mouse sera. Whereas the majority of NSG+hIL6 mice exhibited clear signs of engraftment within 5-10 weeks, by 20 weeks post injection a much smaller fraction of NSG mice scored positive for human Ig serum antibodies, and surprisingly time to

engraftment was especially prolonged for non-conditioned NSG+hIL6 hosts (**Figure 2C**). Although small numbers of human T cells were detected by single cell RNAseq (scRNAseq) (see below), we did not observe clinical signs of graft versus host disease in any mice. Serum protein electrophoresis (SPEP) gels revealed a gamma region M-spike for 9 tested xenografted mice at 15 weeks post injection that was absent in a non-xenografted control (**Figure 2D**). Also consistent with engraftment of monoclonal plasma cells, ELISA for human heavy chains IgG, IgM or IgA showed the presence of only IgG (**Figure 2E**). Staining of BM tissue sections with anti-human CD138 and kappa light chain antibodies revealed clusters of light chain restricted human plasma cells (**Figure 2F**). Flow cytometric analyses of BM cells from serum IgG^+ NSG+hIL6 mice implanted from MM1 showed Igκ restricted light chain expression **(Figure 2G left panel)**, in line with the engrafted myeloma clone. The fraction of all BM cells that were human myeloma cells ranged from <1-12±4%. Consistent with the slow growth rate of malignant plasma cells, under 3% of myeloma cells derived from MM2 engrafted mice were $Ki67^+$ (21) (**Figure 2G right panel**). We concluded that NSG+hIL6 mice with busulfan conditioning were superior in providing a supportive environment for the efficient engraftment and long-term persistence of primary MM cells. Therefore, we used busulfan pre-conditioned NSG+hIL6 mice for all subsequent experiments.

Engraftment of a spectrum of PCDs

Next, we asked whether busulfan pre-conditioned NSG+hIL6 mice support engraftment of other PCDs. With the exception of three samples that were excluded early due to sample mycoplasma contamination, we were able to engraft 100% of NSG+hIL6 mice with 100% of samples from donors experiencing MGUS, smoldering MM, de novo MM, relapsed/refractory (R/R) MM, PCL and AL amyloidosis (**Figure 3A**). This included 100% engraftment of all NSG+hIL6 mice from three cryopreserved relapsed MM or PCL patients from 5 years earlier (**Figure 3A,** asterisks). The ability to

use cryopreserved specimens increases the potential use of this model outside of primary myeloma referral centers.

Flow cytometric analysis of BM from Igλ^+ PCL engrafted mice showed Igλ restricted light chain expression on the BM engrafted clone (**Figure 3B**, left panel). Additionally, Igλ^+ restricted cells dominated the blood (**Figure 3B**, middle panel) and were noted in spleen (**Figure 3B**, right panel). Circulating disease was only detectable in mice engrafted with BM cells from a PCL patient, not other PCDs, in line with observed PCL human phenotypes. Also of note, whereas we often detected surface expression of the ectoenzyme and drug target CD38, its levels varied on the plasma cells derived from different donors (**Figure 3C**). We conclude that the BM microenvironment of NSG+hIL6 mice together with busulfan pre-conditioning supports the engraftment of a wide variety of PCDs with similar disease-affiliated characteristics as their human donors.

Single cell RNAseq analyses

Because we engrafted unsorted BM mononuclear cells from patients with PCDs, we sought to further characterize human cells engrafted into NSG+hIL6 hosts. We performed single cell RNAseq (scRNAseq) on total BM cells from an NSG+hIL6 mouse 52 weeks after implantation with mononuclear BM cells from a patient with IgG lambda R/R MM with t(4;14), sample MM3. We utilized the Parse Biosciences pipeline to prepare and analyze data. Human and mouse cells were distinguished by the presence of species-specific mRNA transcripts. As shown in blue and green (**Figure 4**), human cells comprised a small fraction of total BM cells and segregated into three clusters. These cells included a cluster containing clonal human plasma cells denoted by mRNAs for the IGHG1 and IGL2 genes, the myeloma and plasma cell transcription factors BLIMP1 (22) and IRF4 (23), and the myeloma-associated proteins CD38 (24), CD200 (25), FGFR3 (Fibroblast Growth Factor Receptor-3) and NSD2 (Nuclear receptor binding SET Domain protein-2) (26), the latter two resulting from the t(4;14) translocation present in this patient's myeloma. Additionally, we detected human T cells (CD2$^+$ CD3ε^+) and mast cells

(c-Kit$^+$ GATA2$^+$, IgE Fc receptor subunit β^+). T cells were enriched for transcripts for immune quiescence (TIGIT, LAG3, PD1), and, notably, no graft vs host disease was observed. No human CD34$^+$ stem cell, B-cell (IgM, IgD, PAX5, CD20, CD19), macrophage (CD16, CD14), neutrophil (MPO), megakaryocyte (TPO), stromal cell (FN1, FGFR2), osteoblast (BGLAP, SPP1), eosinophil (ID2) or endothelial cell (CDH5, MCAM) specific markers were detected, arguing against routine engraftment of hematopoietic stem cells. Altogether, based on the results in Figures 1-4 we conclude that NSG+hIL6 mice support the efficient and long-term engraftment of primary PCDs.

Myeloma engrafted NSG+hIL6 mice exhibit signs of disease

To test the utility of NSG+hIL6 mice for study of MM-associated disease states, we probed for signs of urine Ig, anemia, hypercalcemia, MM cell dissemination throughout the skeleton, and bone destruction in mice engrafted with cells from the MM1 or MM2 donor. Due to logistic reasons, not all mice were able to be tested for all clinical sequelae of disease. At 15 weeks post injection, urine from several engrafted mice possessed detectable titers of human Ig (**Figure 5A**), similar to many MM patients. Likewise, RBC counts were significantly lower in serum IgG$^+$ mice compared to non-engrafted controls (**Figure 5B**). Third, though not common, mice with high ionized serum calcium levels were detected in IgG$^+$ mice at levels well above those of non-engrafted mice (**Figure 5C**). Fourth, whereas all mice were inoculated into their left femur, at 8 weeks post-transfer, Igκ$^+$ MM cells were readily detected in both the left (**Figure 5D middle**) and the right femur (**Figure 5D right**), confirming spread within the skeleton, a hallmark of MM.

At 52 weeks, several engrafted mice were assessed for skeletal abnormalities by microCT scan prior to euthanasia. These mice showed thinned bone with vertebral lesions, sternal lesions and even a fractured femur (**Figure 6**). All of these clinical manifestations are commonly observed in advanced human myeloma (27). Together these data indicate that the NSG+hIL6 xenograft model also recapitulates the clinical sequelae of human MM, a feature that heretofore has not been described in

other models. Lastly, majority of engrafted mice succumbed between ~100 and 400 days post-transfer and eventually all mice died. Except for one mouse, all mice died only after detection of circulating Ig, indicating myeloma was responsible for death. The median overall survival of MM1 and MM2 was 296 and 361 days, respectively (**Figure 7**). When cause of death was analyzed, 11 (24%) mice had hind limb paralysis, 16 (35%) became moribund and 14 (30%) were found dead in their cage (**Table 1**).

Responses to anti-myeloma therapies

To test the utility of NSG+hIL6 mice for modeling multiple myeloma therapies, we treated myeloma-engrafted NSG+hIL6 mice with either human BCMA-directed CAR T cells (BCMA-CART cells) (28, 29) or bortezomib. For the BCMA-CART studies, hosts were engrafted with BM cells from a newly diagnosed patient 14-weeks before CAR T cell inoculation, and all hosts possessed human serum IgG within 5 weeks post-engraftment. Each host received $3x10^5$ per dose of untransduced (UTD) or BCMA-CART CD8+ T cells from the same normal donor at “week 0”, and serum human Ig titers traced weekly over the subsequent 6 weeks. Whereas serum IgG levels continued to increase in UTD controls, delivery of BCMA-CART cells coincided with an overall decrease in Ig levels to below detection levels in 5/6 hosts within 2 weeks of BCMA-CART transfer (**Figure 8A**), and an overall relative loss in serum Ig levels compared to UTD controls in every host (**Figure 8B, 8C**). Furthermore, BM $Ig\kappa^+$ MM cells were also significantly depleted in all BCMA CAR T cell treated mice (**Figure 8 D,F**), and as anticipated human $CD8^+$ T cells were readily detected in all hosts (**Figure 8 E,G**).

Additionally, two separate groups of myeloma engrafted mice were treated with saline or bortezomib subcutaneously at 1mg/kg weekly for 4 weeks beginning 30 weeks post-transfer of patient BM cells. Here, we employed a dosing schedule and dose roughly equivalent to a standard one cycle of therapy used for human MM patients. Upon following serum Ig titers weekly for 6 weeks, we observed that bortezomib significantly decreased titers of human IgG compared to saline controls (**Figure 8H**).

We conclude that NSG+hIL6 mice are a highly suitable model system for study of both cellular therapy and small molecule drug candidates in malignant human plasma cells.

Discussion

Our results establish that NSG+hIL6 mice with busulfan conditioning are highly suited for the routine and reproducible engraftment, persistence, and progressive growth of patient-derived malignant plasma cells. Supporting this conclusion, NSG+hIL6 mice were readily engrafted with Ig light chain restricted plasma cells from newly diagnosed and post-relapse myeloma patients as well as donors experiencing MGUS or diagnosed with other plasma cell-driven afflictions including PCL and AL amyloidosis. Further, with time, mouse recipients of myeloma cells experienced progressive increases of human IgG in serum, and many experienced elements of advanced MM such as anemia, hypercalcinemia, bone lesions, and hind limb paralysis consistent with vertebral involvement and cachexia.

Past work has shown that pre-established myeloma cell lines grow rapidly after transfer into NSG mice, often resulting in rapid dominance of host BM within 4 weeks and death soon thereafter (11). By contrast, in NSG+hIL6 mice, patient-derived myeloma cells often comprised a relatively small fraction of all BM cells and appeared to expand relatively slowly, with a median overall survival of 42 or more weeks. Consistent with this conclusion, only small frequencies of Ki67^{+} cells were observed among implanted myeloma cells. The relatively slow growth rates of engrafted plasma cells and the extended survival times of NSG+hIL6 mice are consistent with human disease (21). Indeed, previous attempts to quantify cell division rates for patient myeloma cells suggest relatively slow doubling times ranging from weeks to several months (30, 31). Given that unsorted patient BM mononuclear cells were used for engraftment, we speculate these results suggest that supporting cells may be required for PCD growth in human BM and are either slow growing or altogether absent in many engrafted NSG+hIL6 mice. This hypothesis is further supported by the apparent lack of complete marrow replacement in NSG+hIL6 hosts. scRNAseq of the BM confirmed the presence of the original patient myeloma clone as well as the presence of T cells and mast cells. No other human cell types were detectable by

transcripts. Given the presence of mast cells almost a year after myeloma cell engraftment but a lack of other human myelopoiesis (neutrophils, macrophages in particular), there are likely common myeloid progenitors skewed to mast cell differentiation that were not readily able to be distinguished from the whole human mast cell pool. The presence of T cells likely also indicates a potential imperfect depletion by OKT3 rather than repopulation by human CD34+ stem-like cells, but either way, their level or function are sufficiently low enough that graft vs host disease is not observed. Future serial transplantation studies using NSG+hIL6 transgenic hosts may resolve these issues.

Additional facets of the NSG+hIL6 system are also consistent with human MM. In this regard, we note that disparate clinical phenotypes often developed among cohorts of NSG+hIL6 hosts despite receiving identical doses of donor BM cells on the same day from the same myeloma patient. Indeed, some animals took upwards of 6 months before showing detectable antibody in the blood and became moribund soon thereafter, whereas others harbored readily detectable human IgG titers for months before experiencing clinical symptoms. One possible technical reason is varying amounts of IL-6 between different mice. We neither tracked IL-6 levels during experiments, nor checked IL-6 levels before transplantation of myeloma cells. There is also the possibility that varying phenotypes are not related to IL-6 levels. Human myeloma phenotypes are similarly variable. In this regard, it remains unknown why certain patients develop certain elements of the disease or why some patients' disease remains stable for many years before relapsing while others rapidly progress. Ultimately, our model may provide insights into this problem, thereby leading to a better understanding of how myeloma causes complex clinical phenotypes.

With NSG+hIL6 mice we were able to engraft a diverse set of PCDs in >70% of animals (100% of healthy animals) from both fresh and frozen samples at 5-10 weeks post injection as compared to NSG mice lacking the human IL6 locus. We used death as a read out, which has seldom been done

with past myeloma models, and note that many mice also developed hind limb paralysis at high rates consistent with vertebral involvement and cachexia. Further, longitudinal assay of blood for human antibody titers proved a feasible approach for inferring ongoing treatment response to bortezomib and BCMA CAR-T cell treatment. Further delineation of what cells are responsible for what clinical effects for these and other drugs could lead to development of supportive therapies that prevent myeloma complications in the future.

In summary, we present a new PDX model for PCDs characterized by fidelity to human disease and ease of use. In line with the findings with the MISTRG6 mouse (15), we note dissemination of tumor, circulating disease only with hosts given PCL, and a supportive environment for PCDs in general. The addition of the NSG+hIL6 model and its availability within the research toolbox will aid investigators in the wider PCD research community in the quest for truly durable, curative therapies.

Methods

Sex as a biological variant

Both sexes of mice and patients from which bone marrow samples were procured were used in experiments.

NSG+hIL6 mice

NSG+hIL6 TG mice (Stock# 028655) were imported and are available from Jackson Laboratories (Bar Harbor, ME). To generate NSG+hIL6 mice, a BAC clone (RP11-469J8) carrying a piece of chromosome 7 with the human *IL6* gene and associated promoter and enhancer elements was microinjected into fertilized NSG embryos. All subsequent breeding involved heterozygous males and wild type females, because female NSG+hIL6 mice have low fertility. All mice were bred and maintained under strict clean conditions to minimize risk of infection per protocols within the Penn Stem Cell and Xenograft Core Facility. PCR genotyping for the hIL6 BAC was performed by Transnetyx using the following oligonucleotides: F-GGGAGAGCCAGAACACAGA; R-TGCAGCTTAGGTCGTCATTG.

Study Approval

All human samples were collected after obtaining informed consent per approved IRB protocol # 842940 through the PCD group at the Hospital of the University of Pennsylvania. All mice experiments were performed under the stem cell and xenograft core IACUC protocol for animal model development. Humane endpoints were used to determine when mice were euthanized. These included weight loss >20%, hind limb paralysis, extreme lethargy and respiratory distress.

Preparation of primary human cells

All reagents were dedicated to PC isolation to minimize contamination risk. All parts of this procedure except spinning were done in a tissue culture hood with sufficient laminar air flow. 2-5mL of BM aspirate

was obtained in green top heparin tubes (not EDTA). Aspirate was diluted to 16mL in DPBS with calcium and magnesium (Thermo) in a sterile 50mL conical tube. 4mL of Ficoll Paque plus (Sigma) was carefully added to the bottom of two 15mL conical tubes, then diluted aspirate was carefully layered over the Ficoll. After equally distributing 8mL of diluted aspirate atop each 4mL Ficoll cushion, tubes were carefully capped and moved to a room temperature swinging bucket centrifuge and spun at 700 RCF for 20 minutes without braking. Buffy coats from both tubes were combined into one 50mL conical. 10mL of DPBS with calcium was added and then mixed with inversion before spinning down at 400 RCF for 5 minutes with normal braking parameters. Supernatant was removed and 5mL of ACK lysis buffer (Thermo) was added. Sample was pipetted up and down and allowed to lyse at room temperature for 5 minutes. Cells were spun down and supernatant removed. Cells were resuspended in 1mL of DPBS, mixed with gentle pipetting until single cell suspension and then counted. Total BM mononuclear cells were used for transplantation. If total cell counts were in the millions, cells were frozen or proceeded directly to transplantation. To freeze cells, BM mononuclear cells were counted, spun and resuspended in 1mL cold fetal bovine serum with 10% DMSO in 1-5x10^6 aliquots. Vials were placed in a Corning CoolCell© LX container overnight at -80°C, and the next day samples were moved to a liquid N_2 dewar.

For transplantation, Primocin (Invivogen) was added to the 1mL cell suspension at 100μg/mL along with OKT3 antibody at 10μL/ one million cells and incubated at 4°C for 1 hour as described (32). Antibiotics and OKT3 treatment were performed to decrease risk of infection from donor pathogens into immunodeficient animals and to deplete GvHD causing T cells, respectively. OKT3 does not deplete all T-cells but does prevent GvHD in this model system. A 100μL aliquot was removed and placed at -20ºC for subsequent pathogen testing (IDEXX -hIMPACT panel). Remaining cells were spun down and supernatant removed. Cells were diluted to 1x10^6 cells/10μL/mouse with an extra 10μL overall to account for loss. In small cohorts of mice, there were no differences noted between transplantation of

$5x10^5$, $1x10^6$ or $2x10^6$ mononuclear cells, with a standard dose of $1x10^6$ cells. Cells were transplanted within 4 hours of cell prep completion.

Xenograft transplantation

Mice were conditioned with one intraperitoneal injection of busulfan (30mg/kg) 24 hours prior to introduction of prepared patient BM aspirate. Intraosseous injection of aspirate began with anesthetizing mice using isoflurane on anesthesia nose cone. The injection site used was always the left hind limb. The site was shaved just prior to injection and wiped clean using chlorhexidine wipes x3. Meloxicam or Meloxicam SR was injected prior to incision. The mouse's leg was stabilized in a bent position to allow access to the patellar surface of the femur. A hole is punched through the patellar surface into the shaft of the bone using a 25-gauge needle and then a 30-gauge needle is inserted into the femur. An infusion of 10μL of cells ($1x10^6$ cells/mouse) was administered using a small volume syringe. A drop of vet bond was placed at the insertion site when the needle was withdrawn from the femur. Animals were monitored daily for weight loss, malaise, tumors and limb paralysis. Intravenous injection of patient mononuclear cells was not specifically studied, but preliminary experiments suggest the intraosseous route to be more reliable than intravenous injection.

Following engraftment markers

Blood was the easiest and most reproducible way to follow engraftment of malignant PCs. The NSG mouse has no antibodies at baseline, mouse or human. By following the increase in human titers of total immunoglobulin (Ig) by ELISA it was possible to determine which animals had been engrafted and which had not by ~5 weeks. In high burden states such as PCL, anticoagulated blood is stainable for malignant cells as well. Blood was collected in Eppendorf tubes and allowed to clot for 30 minutes prior to spinning at 8000 RCF for 8 minutes. Serum was then removed to a new tube leaving red cells behind. Sera was then applied to blood and urine ELISA and SPEP as described.

ELISA

ELISA plates (Fisher) were coated using 100μL/well coating buffer ($NaHCO_3$ 2.93g/L, Na_2CO_3 1.59g/L pH 9.6) and 1μg/mL of unlabeled total anti-human total Ig (Southern Biotech) overnight at 4C or at 37C for one hour. Wells were then washed with wash buffer 3 times (1xPBS with 0.1% Tween 20). Blocking buffer (0.22μM filtered 2% BSA in 1xPBS) was added at 100μL/well and allowed to block at room temperature for 1 hour. 1μL of serum from each mouse was added to a single well at the top of a column. Samples were then serially diluted 1:10 down the columns 3 times for a total of 4 wells per samples. This allowed for 24 samples to be run on one plate. Sera were incubated for one hour. Wells were again washed 3 times with wash buffer. Capture buffer (blocking buffer with 1μg/mL of biotin labelled anti-human total Ig) was added to each well at 100μL/well. Plate was incubated at room temperature for 1 hour and then washed again 3 times. 1μL/10mL of streptavidin-HRP was added to each well at 100μL/well and incubated in the dark at room temperature for 1 hour. Wells were again washed 3 times and plate blotted forcefully against paper towels to remove as much wash buffer as possible. Room temperature TMB substrate (Thermo) was prepared and 100uL added to each well. After wells started turning yellow (1-2 minutes or less), reaction was quenched with 200uL of 1M phosphoric acid. Plates were then assessed for absorbance on a Spectramax microplate reader at 450nm with background subtraction at 570nm. For quantification, Ig kappa or lambda monoclonal protein (Thermo) was run at known concentrations at 10-fold dilutions starting at 1000ng down an entire column (7 dilutions x2 columns). Antibody concentrations were determined using 4PL regression in GraphPad Prism 9.

Urine testing for the presence of Ig was also conducted by ELISA with the same method outlined above. Urine was loaded at 10μL into 100μL wells before dilution due to lower concentration of Ig. ELISA testing for hIL-6 was carried out with an hIL-6 kit (R&D DY206).

Histology/Immunohistochemistry (IHC)

Tissues were isolated post euthanasia and placed in 10% formalin overnight at 4C. The next day, fixed tissues were removed to two cassettes per mouse, one for soft tissues and one for bones. These cassettes were then placed in 70% Ethanol/30% water and allowed to soak prior to processing. We utilized the histology services of the UPenn veterinary school for standard practices in decalcification, paraffin block embedding, tissue slice preparation and H&E staining. Slices were put on ProbeOn© (Fisher) slides for IHC.

IHC was performed as per IHC protocol (Abcam). After deparaffinization, slides were submitted to sodium citrate buffer antigen retrieval for 30 minutes prior to overnight incubation of primary antibodies (see **Supplemental Table 1**). 10 minutes of 3% hydrogen peroxide was used to reduce endogenous peroxide background before incubation of secondary HRP conjugated antibody and subsequent DAB substrate application for 12 minutes.

scRNA sequencing of myeloma engrafted BM

BM cells from an NSG+hIL6 mouse engrafted with human myeloma were fixed and stored at -80C with the Evercode cell fixation kit v2 from Parse Biosciences. Just prior to processing, cells were thawed and prepared using the Evercode WT mini v2 kit and associated protocol. This is a plate based barcoding methodology to perform single cell RNA sequencing. Two sublibraries were generated, one with 5000 cells and the second with 10000 cells. Sublibraries were submitted to Azenta Life Sciences for sequencing at equimolar ratios on an Illumina NovaSeq 6000 with paired end 150bp reads (~350 x 10^6 reads). Analysis was performed using the Parse Biosciences platform based in R/Python.

Assaying Serum Ionized Calcium Level

Mouse blood was collected in polypropylene 1.2mL centrifuge tubes without anticoagulants and allowed to clot for 30 minutes prior to spinning at 8000 RCF for 8 minutes and removing the sera to a new tube. Sera were then tested for ionized calcium concentration using the Calcium Assay Kit (Abcam 102505).

Serum Protein Electrophoresis (SPEP)

SPEP was carried out using the QuickGel station from Helena Laboratories and the Split-Beta SPE Kit (3550T) per manufacturer's instructions.

Complete Blood Counts

At 15 weeks post injection of patient samples from MM1 and MM2, blood was collected in EDTA coated vacutainer tubes and sent to IDEXX analytics for formal complete blood count testing (test code 375).

MicroCT scanning

With the help of the Small Animal Imaging Facility Core Resource at UPenn, mice were anesthetized using inductive isoflurane and then maintained through nose cone prior to mounting on the MILabs U-CT ultra-high resolution (~20 µm) small-to-medium sized animal CT scanner. 4-minute scans were obtained prior to euthanasia. Images were analyzed using ImageJ.

Flow Cytometry

Cells were isolated from femurs and spleens on ice, lysed for red blood cells using ACK lysis buffer (Thermo) for 5 minutes at room temperature and then stained for live cells with zombie aqua live/dead (Thermo) (10 minutes) and fluorescently labeled antibodies of markers of interest (30 minutes) in 0.1%BSA PBS buffer. Please see **Supplemental Table 1** for antibodies used.

Statistics

2-sided ANOVA and appropriate single or multiple comparison t-tests were used and calculated with GraphPad Prism. Specific tests are denoted in figure legends. All summary data points are means, and all error bars denote standard deviation. Significance cut offs were α=0.05. P value less than 0.05 was considered significant. Cohorts MM1 and MM2 were powered at 80% under the assumption that NSG+hIL6 mice would have an engraftment incidence of 80% based upon observed engraftment in the MISTRG6 model vs. 20% in NSG mice from our prior experience. Treatment with bortezomib could not be powered to the same level given the lack of available myeloma engrafted mice at the time of experimentation. Unless otherwise stated in figure legends, all displayed experiments were performed once but used only biological replicates (each data point represents a unique mouse).

BCMA CAR T cells

CAR T-cells specific for BCMA were kindly provided by the Posey & Milone labs at the University of Pennsylvania. The BCMA single chain variable fragment employed for BCMA-CART cells was also used in a clinical trial for relapsed refractory myeloma (29) and consists of Ig heavy and light chain variable regions derived from a BCMA-reactive antibody ("clone 10") assembled with an extracellular hinge and transmembrane region derived from CD8 linked to an intracellular signaling cassette derived from CD3ζ and a 4-1BB intracellular domain as described (28). PCR-amplified CAR constructs were subcloned into the pTRPE vector before packaging into lentivirus using a VSVG envelope and HEK293T cells. Patient T cells were stimulated and treated with CAR containing lentivirus, then expanded and harvested for injection at 3 x 10^5 cells/mouse.

Data Availability

Single cell RNA sequencing data has been uploaded to the NCBI GEO database with accession numbers GSE246140, GSM7857100 and GSM785710. Both raw data files as well as normalized files from which the analyses within this manuscript were derived are available for download. Code for

scRNA analysis is available from Parse Biosciences. Supporting data values for all figures were submitted to JCI Insight and are available for download.

Author Contributions

ZSH designed and performed experiments, analyzed data, and wrote the manuscript. AG provided patient samples and wrote the manuscript. LB and LDS designed and performed experiments. YT, SK, WL and NCS designed and performed experiments. DD performed experiments. DTV, ADC, AJW and SPS provided patients samples and reviewed the manuscript. MC and EAS designed experiments and wrote the manuscript. DA designed experiments, analyzed data and wrote the manuscript.

Acknowledgements

We thank members of the Stem Cell and Xenograft Core of the Perelman School of Medicine (SCR_010035), Flow Cytometry and Cell Sorting Core Resource Facility, Human Immunology Core, Small Animal Imaging Facility Core and Comparative Pathology Core and PennVet Comparative Histology Core. This work was supported by an ASPIRE award from the Mark Foundation for Cancer Research (DA), National Institutes of Health (NIH) training grant T32-HL07439 (ZH), a pilot grant from the Abramson Cancer Center Core (P30) (ZSH, DA), the Kohler Drennan Fund for Multiple Myeloma Research (ZH,AG,ES), the Hematologic Malignancies Translational Center of Excellence (MC, ES), an LLS Scholar award in Clinical Research (AG), an Amyloidosis Foundation Research Grant (ZH) and NIH grants RO1 AI139123 and RO1 AI175185 (DA) and CA034196 (LDS). Dr. Carroll receives salary support from VA Merit Award, 5 I01 BX004662.

References

1. Ludwig H, Novis Durie S, Meckl A, Hinke A, and Durie B. Multiple Myeloma Incidence and Mortality Around the Globe; Interrelations Between Health Access and Quality, Economic Resources, and Patient Empowerment. *Oncologist.* 2020;25(9):e1406-e13.
2. Weiss BM, Abadie J, Verma P, Howard RS, and Kuehl WM. A monoclonal gammopathy precedes multiple myeloma in most patients. *Blood.* 2009;113(22):5418-22.
3. Tuazon SA, Holmberg LA, Nadeem O, and Richardson PG. A clinical perspective on plasma cell leukemia; current status and future directions. *Blood Cancer J.* 2021;11(2):23.
4. Gertz MA. Immunoglobulin light chain amyloidosis: 2022 update on diagnosis, prognosis, and treatment. *Am J Hematol.* 2022;97(6):818-29.
5. Durie BGM, Hoering A, Abidi MH, Rajkumar SV, Epstein J, Kahanic SP, et al. Bortezomib with lenalidomide and dexamethasone versus lenalidomide and dexamethasone alone in patients with newly diagnosed myeloma without intent for immediate autologous stem-cell transplant (SWOG S0777): a randomised, open-label, phase 3 trial. *Lancet.* 2017;389(10068):519-27.
6. Benboubker L, Dimopoulos MA, Dispenzieri A, Catalano J, Belch AR, Cavo M, et al. Lenalidomide and dexamethasone in transplant-ineligible patients with myeloma. *N Engl J Med.* 2014;371(10):906-17.
7. van de Donk N, Pawlyn C, and Yong KL. Multiple myeloma. *Lancet.* 2021;397(10272):410-27.
8. Lawson MA, Paton-Hough JM, Evans HR, Walker RE, Harris W, Ratnabalan D, et al. NOD/SCID-GAMMA mice are an ideal strain to assess the efficacy of therapeutic agents used in the treatment of myeloma bone disease. *PLoS One.* 2015;10(3):e0119546.
9. Neri P, Tagliaferri P, Di Martino MT, Calimeri T, Amodio N, Bulotta A, et al. In vivo anti-myeloma activity and modulation of gene expression profile induced by valproic acid, a histone deacetylase inhibitor. *Br J Haematol.* 2008;143(4):520-31.
10. Mitsiades CS, Mitsiades NS, Bronson RT, Chauhan D, Munshi N, Treon SP, et al. Fluorescence imaging of multiple myeloma cells in a clinically relevant SCID/NOD in vivo model: biologic and clinical implications. *Cancer research.* 2003;63(20):6689-96.
11. Sarin V, Yu K, Ferguson ID, Gugliemini O, Nix MA, Hann B, et al. Evaluating the efficacy of multiple myeloma cell lines as models for patient tumors via transcriptomic correlation analysis. *Leukemia.* 2020;34(10):2754-65.
12. Tsunenari T, Koishihara Y, Nakamura A, Moriya M, Ohkawa H, Goto H, et al. New xenograft model of multiple myeloma and efficacy of a humanized antibody against human interleukin-6 receptor. *Blood.* 1997;90(6):2437-44.
13. Yata K, and Yaccoby S. The SCID-rab model: a novel in vivo system for primary human myeloma demonstrating growth of CD138-expressing malignant cells. *Leukemia.* 2004;18(11):1891-7.

14. Schueler J, Wider D, Klingner K, Siegers GM, May AM, Wasch R, et al. Intratibial injection of human multiple myeloma cells in NOD/SCID IL-2Rgamma(null) mice mimics human myeloma and serves as a valuable tool for the development of anticancer strategies. *PLoS One.* 2013;8(11):e79939.
15. Das R, Strowig T, Verma R, Koduru S, Hafemann A, Hopf S, et al. Microenvironment-dependent growth of preneoplastic and malignant plasma cells in humanized mice. *Nat Med.* 2016;22(11):1351-7.
16. Hammacher A, Ward LD, Weinstock J, Treutlein H, Yasukawa K, and Simpson RJ. Structure-function analysis of human IL-6: identification of two distinct regions that are important for receptor binding. *Protein Sci.* 1994;3(12):2280-93.
17. Ono R, Watanabe T, Kawakami E, Iwasaki M, Tomizawa-Murasawa M, Matsuda M, et al. Co-activation of macrophages and T cells contribute to chronic GVHD in human IL-6 transgenic humanised mouse model. *EBioMedicine.* 2019;41:584-96.
18. Said EA, Al-Reesi I, Al-Shizawi N, Jaju S, Al-Balushi MS, Koh CY, et al. Defining IL-6 levels in healthy individuals: A meta-analysis. *Journal of medical virology.* 2021;93(6):3915-24.
19. Nachbaur DM, Herold M, Maneschg A, and Huber H. Serum levels of interleukin-6 in multiple myeloma and other hematological disorders: correlation with disease activity and other prognostic parameters. *Ann Hematol.* 1991;62(2-3):54-8.
20. Peake K, Manning J, Lewis CA, Barr C, Rossi F, and Krieger C. Busulfan as a myelosuppressive agent for generating stable high-level bone marrow chimerism in mice. *J Vis Exp.* 2015(98):e52553.
21. Gastinne T, Leleu X, Duhamel A, Moreau AS, Franck G, Andrieux J, et al. Plasma cell growth fraction using Ki-67 antigen expression identifies a subgroup of multiple myeloma patients displaying short survival within the ISS stage I. *Eur J Haematol.* 2007;79(4):297-304.
22. Shapiro-Shelef M, Lin KI, McHeyzer-Williams LJ, Liao J, McHeyzer-Williams MG, and Calame K. Blimp-1 is required for the formation of immunoglobulin secreting plasma cells and pre-plasma memory B cells. *Immunity.* 2003;19(4):607-20.
23. Shaffer AL, Emre NC, Lamy L, Ngo VN, Wright G, Xiao W, et al. IRF4 addiction in multiple myeloma. *Nature.* 2008;454(7201):226-31.
24. Costa F, Dalla Palma B, and Giuliani N. CD38 Expression by Myeloma Cells and Its Role in the Context of Bone Marrow Microenvironment: Modulation by Therapeutic Agents. *Cells.* 2019;8(12).
25. Moreaux J, Hose D, Reme T, Jourdan E, Hundemer M, Legouffe E, et al. CD200 is a new prognostic factor in multiple myeloma. *Blood.* 2006;108(13):4194-7.
26. Kalff A, and Spencer A. The t(4;14) translocation and FGFR3 overexpression in multiple myeloma: prognostic implications and current clinical strategies. *Blood Cancer J.* 2012;2(9):e89.
27. Hameed A, Brady JJ, Dowling P, Clynes M, and O'Gorman P. Bone disease in multiple myeloma: pathophysiology and management. *Cancer Growth Metastasis.* 2014;7:33-42.
28. Bu DX, Singh R, Choi EE, Ruella M, Nunez-Cruz S, Mansfield KG, et al. Pre-clinical validation of B cell maturation antigen (BCMA) as a target for T cell immunotherapy of multiple myeloma. *Oncotarget.* 2018;9(40):25764-80.

29. Cohen AD, Garfall AL, Stadtmauer EA, Melenhorst JJ, Lacey SF, Lancaster E, et al. B cell maturation antigen-specific CAR T cells are clinically active in multiple myeloma. *J Clin Invest.* 2019;129(6):2210-21.

30. Drewinko B, Alexanian R, Boyer H, Barlogie B, and Rubinow SI. The growth fraction of human myeloma cells. *Blood.* 1981;57(2):333-8.

31. Hokanson JA, Brown BW, Thompson JR, Drewinko B, and Alexanian R. Tumor growth patterns in multiple myeloma. *Cancer.* 1977;39(3):1077-84.

32. Wunderlich M, Brooks RA, Panchal R, Rhyasen GW, Danet-Desnoyers G, and Mulloy JC. OKT3 prevents xenogeneic GVHD and allows reliable xenograft initiation from unfractionated human hematopoietic tissues. *Blood.* 2014;123(24):e134-44.

Figure Legends:

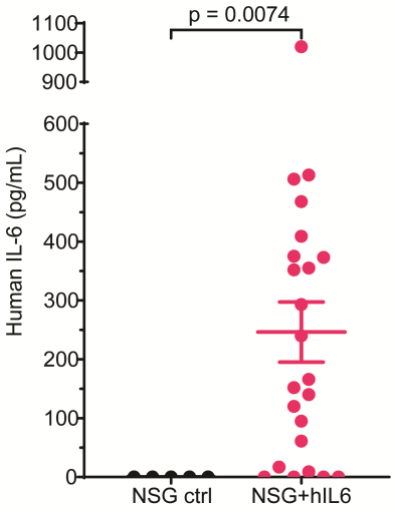

Figure 1: Human IL-6 in NSG+hIL6 sera. Sera from 12–20-week-old NSG (n=5) and NSG+hIL6 (n=23) mice were evaluated for human IL-6 levels by quantitative ELISA. Horizonal lines and error bars indicate the mean and the standard deviation of the mean, respectively. Statistics were calculated with the Kolmogorov-Smirnov comparison.

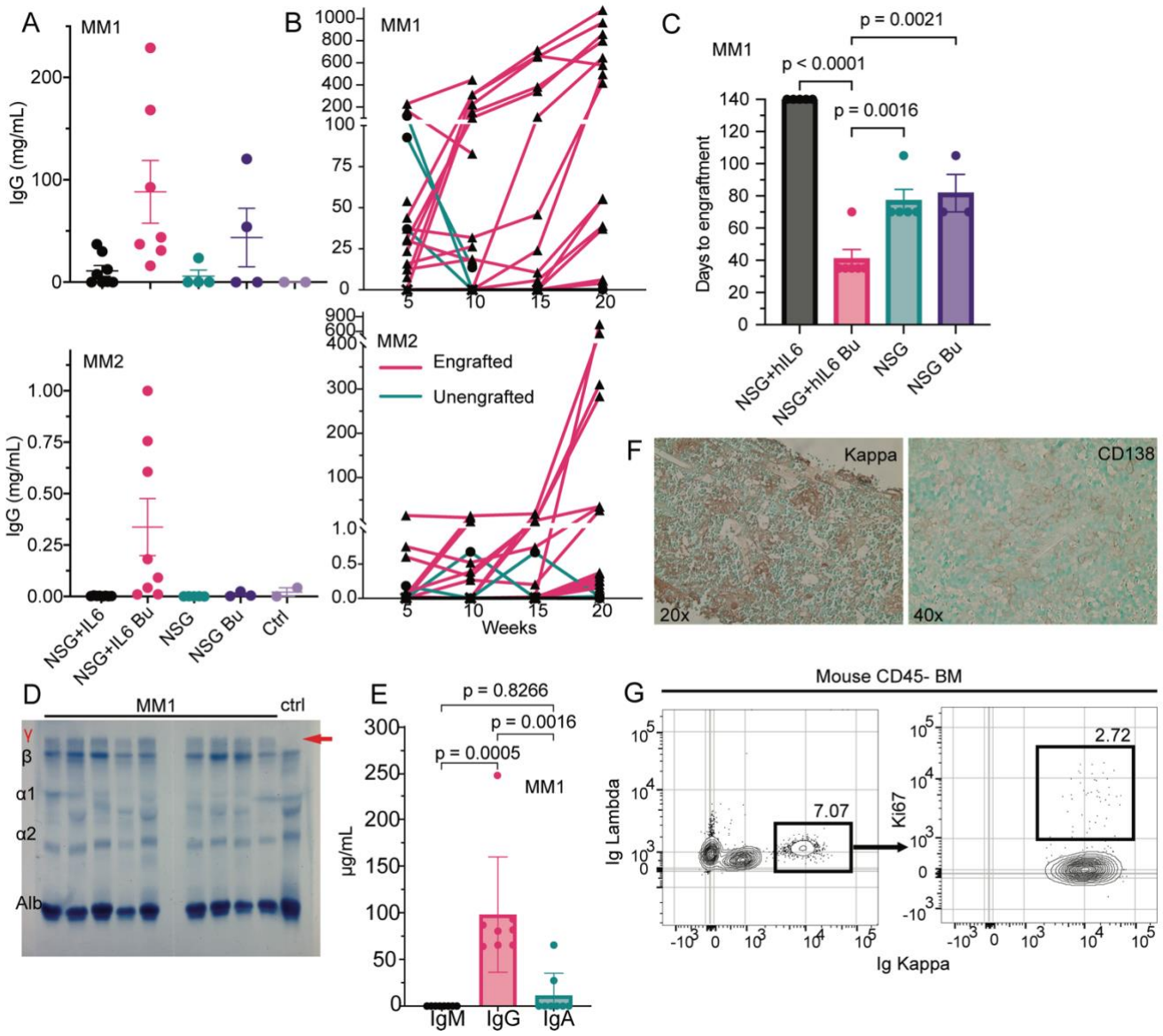

Figure 2: NSG+hIL6 mice support primary patient MM. BM cells from one of two newly diagnosed MM patients ("MM1" and "MM2") were transferred via intraosseous injection to NSG or NSG+hIL6 adults with and without busulfan pretreatment. MM1: NSG+IL6 (n=8), NSG+IL6 busulfan (n=7), NSG (n=4), NSG busulfan (n=4); MM2: NSG+IL6 (n=7), NSG+IL6 busulfan (n=8), NSG (n=5), NSG busulfan (n=3); No myeloma control (n=2). (A) Sera from the indicated cohorts were evaluated for human IgG levels by ELISA 5 weeks post injection. "Ctrl" indicates saline injected NSG+hIL6 mice. Horizonal lines and error bars indicate the mean and standard deviation of the mean, respectively. (B) Serum IgG levels in MM1 and MM2 engrafted mice over 20 weeks grouped by engraftment status (unengrafted: green line and

circle, engrafted: pink line and triangle). (C) Time to detection of serum human Ig (functional engraftment) for NSG vs NSG+hIL6 hosts with or without preconditioning with MM1 (NSG-hIL6 Bu vs NSG ($p=0.0016$), NSG-hIL6 ($p<0.0001$), NSG Bu ($p=0.0021$)). Each data point represents a single mouse. (D) SPEP analysis (n=9) of sera samples from mice engrafted with MM1 vs an unengrafted control (n=1). Gamma region denoted with the red γ. Red arrow denotes M-spike representative of myeloma engraftment. (E) Total IgM, IgG and IgA serum levels (n=7) from mice engrafted with MM1 were determined by ELISA. (F) Histologic sections prepared from the BM of an MM1 engrafted NSG+hIL6 host were stained with antibodies specific for human Ig kappa or CD138. (G) BM cells from an MM1 engrafted NSG+hIL6 host were pre-gated on viable mouse CD45-, human CD3- CD20- cells evaluated for intracellular Igκ and Igλ and Ki-67 expression. Statistics for (C) and (E) were calculated using Dunnett's multiple comparisons test and Tukey's multiple comparisons test respectively. (F) is representative of similarly observed findings from 12 mice.

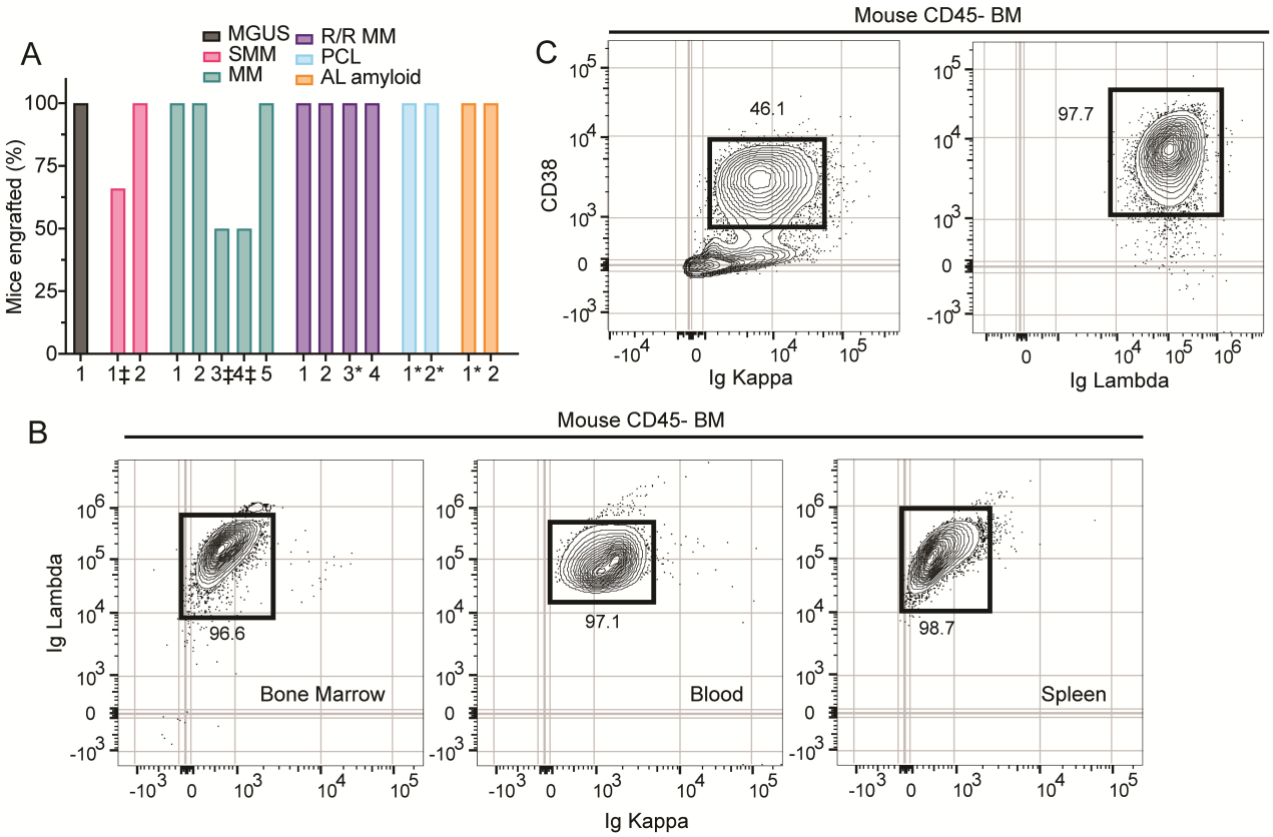

Figure 3: NSG+hIL6 mice support major plasma cell dyscrasias. NSG+hIL6 mice served as hosts for BM cells derived from patients with MGUS (n=1), smoldering multiple myeloma (SMM) (n=2), newly diagnosed multiple myeloma (MM) (n=5), relapsed/refractory myeloma (R/R MM) (n=4), plasma cell leukemia (PCL) (n=2), or AL amyloidosis (AL amyloid) (n=2). (A) Shown is the fraction of mice in each cohort with sera scoring positive for human IgG patients at 10 weeks post-transfer. (n=5 hosts/grp). *Recipients of previously frozen human BM cells. ‡ Samples not reaching 100% engraftment were prematurely terminated after 3 weeks due to mycoplasma contamination. (B) Flow cytometric analysis for Ig lambda and Ig kappa expression in permeabilized mouse BM (left), blood (middle) and spleen (right) cells harvested from an NSG+hIL6 mouse engrafted with BM from a PCL patient. (C) Analysis of CD38 and Ig kappa or Ig lambda expression for mouse BM cells from separate NSG+hIL6 hosts engrafted previously with BM cells from the MM2 donor (left) or the PCL patient illustrated in (B). For (B) and (C) plots were gated on viable mouse CD45 negative singlets.

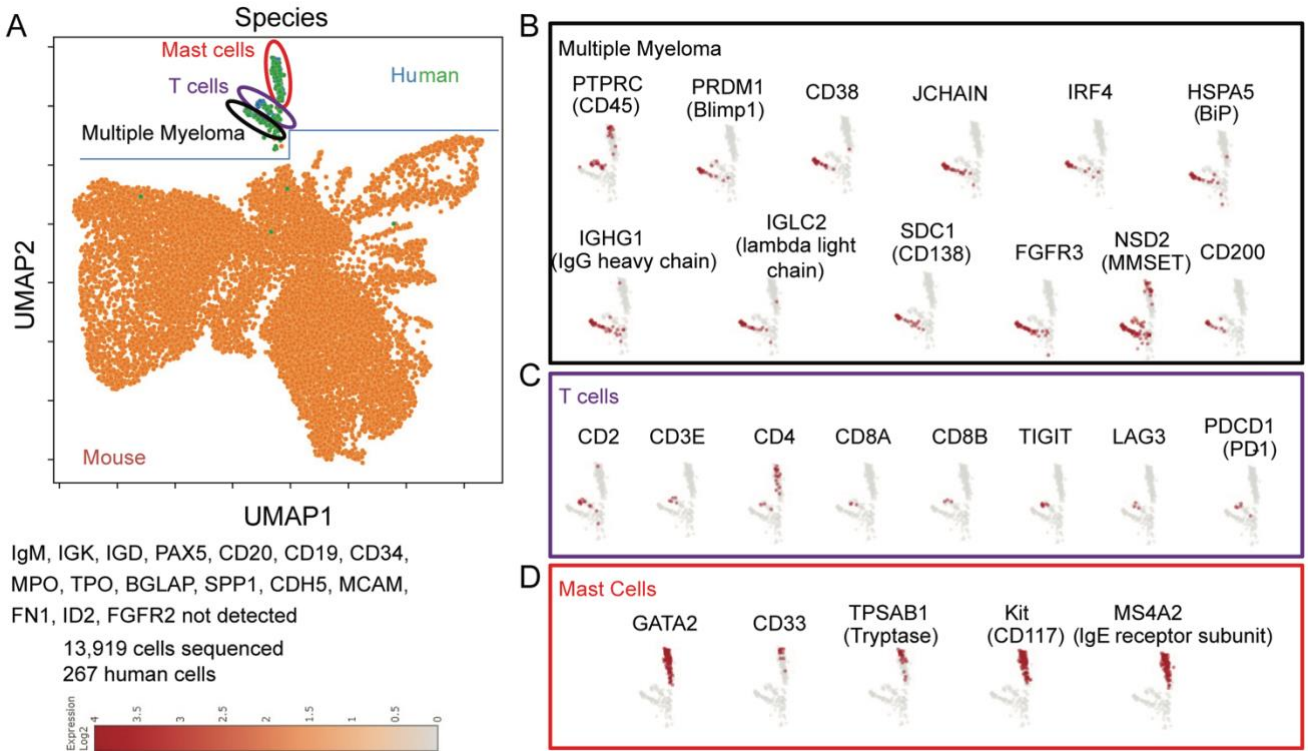

Figure 4: Characterization of NSG+hIL6 mice engrafted mice. BM from an NSG+hIL6 mouse engrafted with mononuclear human BM cells from patient sample R/R MM3 was isolated 52 weeks after intraosseous injection and subjected to scRNAseq using the Parse Biosciences processing and analysis pipeline. (A) UMAP denotes the presence of mouse cells (orange) and human cells (green and blue). Human cells form 3 clusters. Gene expression profiles define these as (B) myeloma cells (black), (C) T cells (purple) and (D) mast cells (red). The data herein represent scRNAseq from one mouse engrafted with one human myeloma sample.

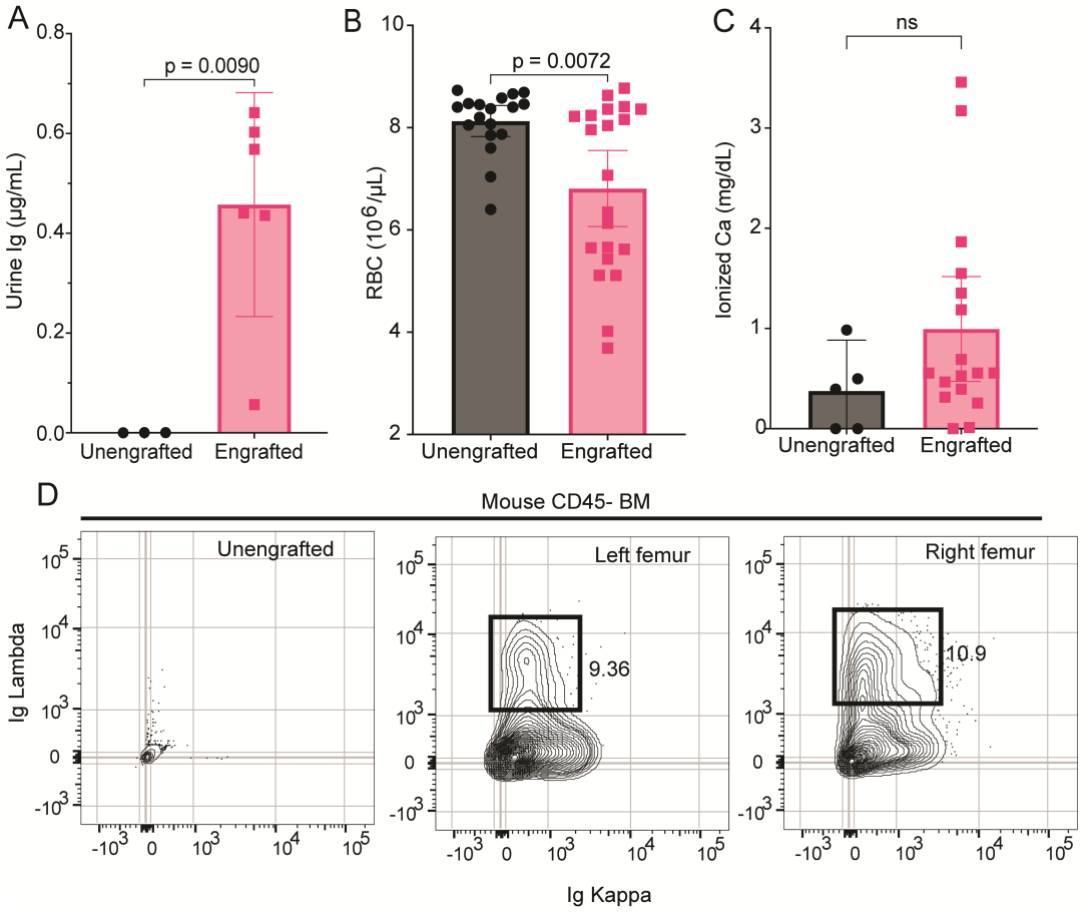

Figure 5: Myeloma engrafted NSG+hIL6 mice with sequelae of human disease. (A) Urine from NSG+hIL6 mice (n=6) engrafted 15 weeks previously with MM1 BM cells and unengrafted controls (n=3) was evaluated for human Ig. (B) RBC counts from engrafted (n=18) vs. unengrafted (n=21) mice at 15 weeks post injection. (C) Serum ionized calcium concentrations in engrafted (n=15) compared to unengrafted controls (n=5) at 15 weeks. (D) Flow cytometric analysis of Ig kappa and Ig lambda expression for permeabilized BM cells from an unengrafted NSG+hIL6 mouse (left plot), the left femur (middle plot) and right femur (right plot) of a serum human IgG^+ NSG+hIL6 mouse given MM1 BM cells 12 weeks previously. BM cells were only injected into the left femur. Columns and error bars indicate the mean and standard deviation of the mean, respectively. Statistics were calculated with Mann-Whitney t-tests. Flow images in (D) are representative of 12 mice with similar findings.

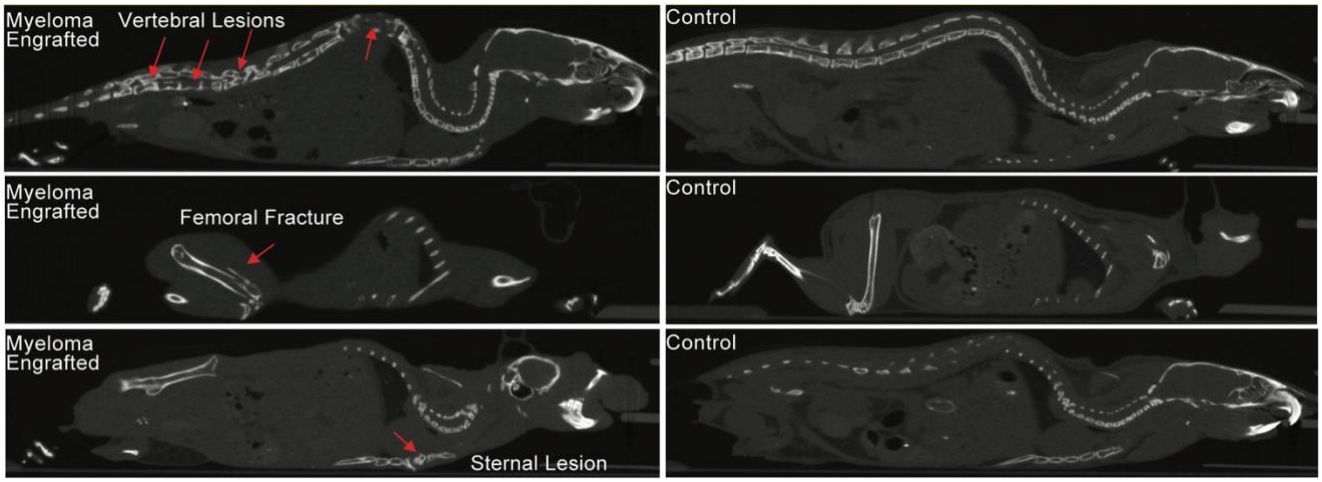

Figure 6: Myeloma engrafted NSG+hIL6 mice develop skeletal lesions. Computed tomography (CT) scans of surviving human IgG^{+} NSG+hIL6 were performed at 52 weeks post injection. Vertebral (top left), femoral (middle left) and sternal (bottom left) lytic lesions in MM1 and MM2 engrafted mice (red arrows) were noted compared to NSG+hIL6 mice not engrafted with MM. Lesions are representative of 14 imaged animals.

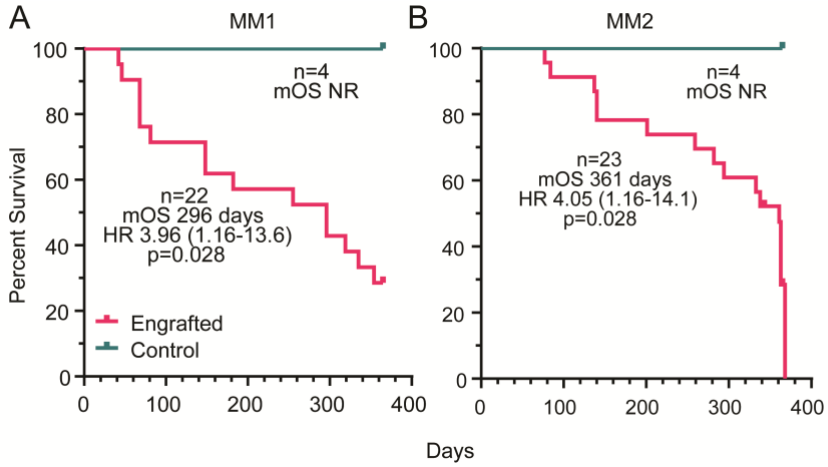

Figure 7: Mortality of myeloma engrafted NSG+hIL6 mice. Kaplan-Meier curves for NSG+hIL6 mice that were engrafted at 16-weeks of age with BM cells from donor MM1 (engrafted (n=22); unengrafted (n=4)) (A) or MM2 (engrafted (n=23); unengrafted (n=4)) (B). All mice were monitored for humane endpoints over the indicated time frames. There was only a single mouse, within the MM1 cohort, that was injected with myeloma cells and died before IgG was detectable in the serum. All others had detectable IgG at the time of death. Statistics were calculated with Log rank Mantel Cox testing.

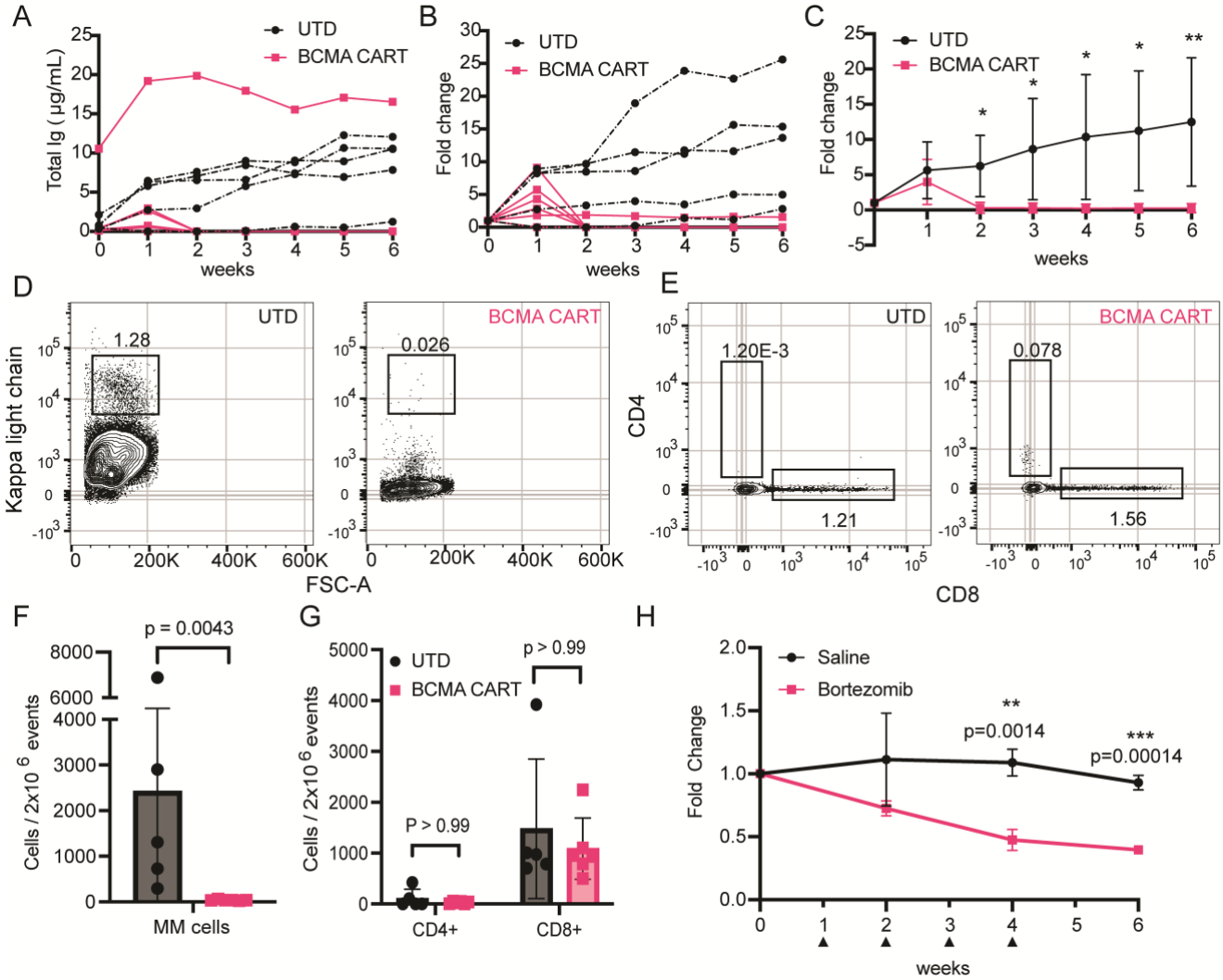

Figure 8: Responses to BCMA-CART or bortezomib. (A-G) NSG+hIL6 mice were implanted with BM cells from an untreated newly diagnosed Igκ^{+} MM patient. 14 weeks later ("week zero") serum Ig+ mice were given a single dose of human BCMA-CART cells (pink, n=6) or untransduced T-cells (UTD) from the same normal donor (black, n=5). Sera were assayed by ELISA for human Ig weekly over 6 weeks (A-C). Shown are total Ig levels (A), fold change over time (B), and aggregate fold change data for each group (C). For (A) and (B) each line derives from an individual host. For (C) *p<0.05, **p<0.005. (D, E) Representative flow cytometric plots on week 6 for Igκ^{+} (D) or CD4+ and CD8^{+} T cells (E) BM cells in recipients of UTD or BCMA-CART cells as indicated. Igκ v FSC plots are pre-gated on viable CD19^{-}, CD3^{-} events; CD4 vs CD8 T cell plots are pre-gated on viable CD3^{+} events. (F, G) Means and standard

deviations for Igk$^+$ (F) or CD8$^+$ T cells (G) in on week 6. (H) Separate experiment wherein serum human IgG$^+$ NSG+hIL6 mice were given 4 doses (black arrowheads) of saline (black, n=3, 10uL/g) or bortezomib (red, n=3, 1mg/kg IV) over four weeks. Statistics were calculated with Mann-Whitney t-tests.

Tables:

MM1							
	Cause of death	Survival (days)	Sex	Hypercalcemia	Urine light chains	Anemia	Bone lesions (~52 weeks)
NSG							
2428	end of study	397	F			no	
2436	found dead	255	F		yes	no	
2439	moribund	255	M		no	no	yes
2444	hind limb paralysis	255	F	no		no	
NSG IL6							
2412	moribund	148	M			no	
2414	censored, death with anesthesia		M		yes	no	
2417	moribund	255	M			yes	
2418	found dead	319	F	no		no	
2421	moribund	296	F			no	
2437	moribund	182	F	no		yes	
2443	found dead	81	F				
2447	found dead	354	F	yes		no	
NSG Busulfan							
2416	moribund	51	M				
2420	hind limb paralysis	296	F			no	
2435	hind limb paralysis	335	F			yes	yes
2442	found dead	46	F				
NSG IL6 Busulfan							
2411	found dead	42	M				
2413	moribund	148	M			yes	
2415	moribund, massive ascites	68	M		no		
2427	hind limb paralysis	397	F		yes	yes	
2438	moribund	68	F	no			
2441	moribund	296	M		yes	yes	
2445	moribund	68	F				

Table 1: Characteristics of MM1 and MM2 engrafted NSG+hIL6 mice

MM2							
	Cause of death	Survival (days)	Sex	Hypercalcemia	Urine light chains	Anemia	Bone lesions (~52 weeks)
NSG							
2802	hind limb paralysis	137	M		yes	no	
2804	hind limb paralysis	201	M			yes	
2810	end of study	397	F			no	
2813	moribund	140	M			no	
2818	moribund, massive ascites	333	F	yes		no	yes
NSG IL6							
2823	found dead	361	F			no	
2832	found dead	338	F			no	
2828	moribund	363	M	yes		no	yes
2829	censored, death from anesthesia		M			no	
2837	end of study	397	M	yes	no	no	
2825	found dead	368	M	yes		no	
2817	end of study	397	F			no	
2821	found dead	282	F	no		no	
NSG Busulfan							
2807	hind limb paralysis	294	F	yes		yes	
2808	moribund	77	F				
2801	hind limb paralysis	333	M			no	
NSG-IL6 Busulfan							
2803	moribund	363	M			no	yes
2805	moribund	84	M		yes		
2806	hind limb paralysis	363	F			yes	yes
2809	hind limb paralysis	363	F			no	yes
2811	end of study	397	F		yes	yes	
2812	moribund	140	F			yes	
2814	hind limb paralysis	259	M			yes	

Table 1: Characteristics of MM1 and MM2 engrafted NSG+hIL6 mice (continued)